

Prefix-tree Decoding for Predicting Mass Spectra from Molecules

Samuel Goldman
Computational and Systems Biology
MIT
Cambridge, MA 02139
samlg@mit.edu

John Bradshaw
Chemical Engineering
MIT
Cambridge, MA 02139
jbrad@mit.edu

Jiayi Xin
Statistics and Actuarial Science
The University of Hong Kong
Pokfulam, Hong Kong
xinjiayi@connect.hku.hk

Connor W. Coley
Chemical Engineering
Electrical Engineering and Computer Science
MIT
Cambridge, MA 02139
ccoley@mit.edu

Abstract

Computational predictions of mass spectra from molecules have enabled the discovery of clinically relevant metabolites. However, such predictive tools are still limited as they occupy one of two extremes, either operating (a) by fragmenting molecules combinatorially with overly rigid constraints on potential rearrangements and poor time complexity or (b) by decoding lossy and nonphysical discretized spectra vectors. In this work, we introduce a new intermediate strategy for predicting mass spectra from molecules by treating mass spectra as sets of chemical formulae, which are themselves multisets of atoms. After first encoding an input molecular graph, we decode a set of chemical subformulae, each of which specify a predicted peak in the mass spectra, the intensities of which are predicted by a second model. Our key insight is to overcome the combinatorial possibilities for chemical subformulae by decoding the formula set using a prefix tree structure, atom-type by atom-type, representing a general method for ordered multiset decoding. We show promising empirical results on mass spectra prediction tasks.

1 Introduction

As the primary tool to discover unknown small molecule structures from biological samples, tandem mass spectrometry (MS/MS) experiments have enabled the identification of numerous important molecules implicated in health and disease [4, 34, 47]. Tandem mass spectrometers are capable of isolating, fragmenting, and measuring the resulting fragment masses of small molecules from a sample, producing a signature (a mass spectrum) for each detected molecule (Figure 1, top).

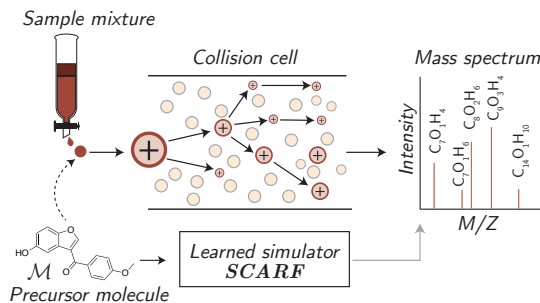


Figure 1: Tandem mass spectrometers measure fragmentation patterns of molecules, resulting in characteristic peaks that are diagnostic of their structure. SCARF simulates these fragmentation patterns *in silico*.

Computationally predicting mass spectra from molecules *in silico* (Figure 1, bottom) is thus a longstanding and important challenge. Not only does this assist practitioners in better understanding the fragmentation process, but it also enables the identification of molecules from newly observed spectra by comparing an observed spectrum to virtual spectra generated from a database of candidate molecules. While a large library of empirical mass spectra could theoretically serve the same purpose, the size of such libraries is limited by the slow and expensive process of acquiring pure chemical standards and measuring their spectra, motivating computational prediction.

We argue that there are three core desiderata for a forward molecule-to-spectrum simulation model, or “spectrum predictor”. An ideal spectrum predictor should be (i) *accurate*, being able to predict the exact set of fragment masses and intensities with a precision comparable to experimental measurements; (ii) *physically-inspired*, to avoid making physically nonsensical (“invalid”) suggestions and to provide interpretations of the chemical species for each peak; and (iii) *fast*, such that it is computationally inexpensive to predict spectra for many (e.g., millions) hypothetical molecules.

Unfortunately, many existing spectrum predictors do not meet these criteria. Methods to date have tended to follow one of two approaches: (a) physically-motivated fragmentation approaches or (b) molecule-to-vector (or “binned”) approaches (Figure 2A-B). Fragmentation approaches (e.g., 2, 17, 36, 48) take an input molecule and suggest bonds that may break, creating fragments that are scored by ML algorithms or curated rulesets (Figure 2A). While interpretable, these methods are often slow and restrictive; certain mass spectrum peaks are generated by complex chemical rearrangements within the collision cell that cannot be approximated by bond breaking alone. That is, observed fragments are not contiguous substructures of the original molecule [9, 11]. On the other hand, binned prediction approaches (e.g., 46, 51, 54) are less physically-grounded, using neural networks to directly learn a mapping from molecules to vectors representing discretized versions of the spectra (Figure 2B). These methods, while fast, lack interpretability and due to discretization have a mass precision lower than that of most modern spectrometers, limiting their accuracy.

We propose to address the shortcomings of previous work by predicting mass spectra from molecules at the level of chemical formulae (e.g., $C_xN_yO_zH_w\dots$) and introduce a new method, Subformulae Classification for Autoregressively Reconstructing Fragmentations (SCARF) to do so. Because the chemical formula for each input molecule is known, each subformula in the predicted set of peaks is constrained to contain a subset of the atoms in the original formula. Our primary contributions are:

- posing mass spectrum prediction as a two step process: first generating the set of chemical formulae for the fragments, then associating these formulae with intensities;
- overcoming the combinatorial subformula option space by learning to generate formula prefix trees;
- demonstrating the empirical benefit of SCARF in predicting experimental mass spectra quickly and accurately using two separate datasets.

2 Background

We provide a short introduction of tandem mass spectrometry suitable for a general machine learning audience, detail previous approaches to modeling this process as they relate to our proposed approach SCARF, and explain how such tools can be utilized to discover molecules from new spectra. We refer interested readers to [23] for further details on the physical process of mass spectrometry.

2.1 Tandem mass spectrometry

Tandem mass spectrometers (MS/MS) measure fragmentation patterns of molecules in a multi-stage process. The input to the process is a solution containing a *precursor* molecule, $\mathcal{M} \in \mathcal{X}$, associated with a chemical formula, \mathcal{F} , defining the counts of each element present; for instance $\mathcal{F} = C_{16}O_4H_{12}$ for the precursor molecule shown in Figure 1. The precursor molecule is first ionized (i.e., made charged), often by bonding or associating with an *adduct* (e.g., a proton, H^+) present in the solution. The charged product is then measured by a mass analyzer (MS1), where its mass-to-charge ratio (m/z) is measured.

This precursor ion is then filtered into a *collision cell*. Here, through interactions with an inert gas, the precursor ion is broken down into a set of one or more *product ions*, each of which is associated with

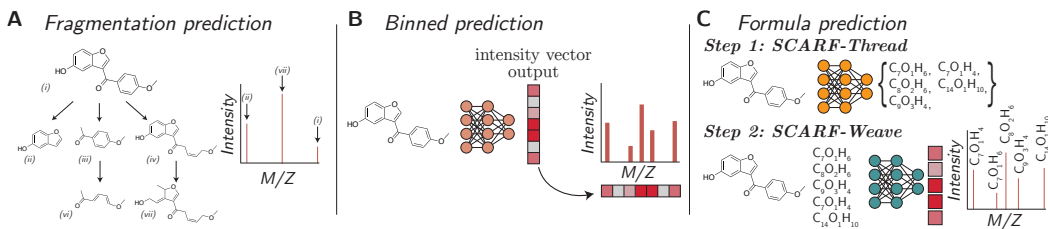


Figure 2: Overview of various approaches to spectrum prediction. **A.** Fragmentation prediction approaches use heuristics and scoring rules to break down the molecule into fragments and their associated intensities. **B.** Binned prediction approaches discretize the possible mass-to-charge values and predict intensities for each possible bin. **C.** Formula prediction approaches predict spectra as sets of chemical formulae and intensities. Our model SCARF utilizes a two stage approach, first by predicting the product formulae present (constrained by the precursor formula), which defines the x-axis locations of the peaks, before secondly assigning intensities to these formulae (defining the peaks’ y-axis values).

a new chemical formula; for example, one might be $f^1 = C_7OH_4$ for the process shown in Figure 1. Finally, this set of product ions is measured by a second mass analyzer (MS2), along with the set of their intensities, $y^i \in \mathbb{R}^+$ (i.e., relative frequency over several repetitions of this process), creating what is referred to as a *peak*. The collection of all peaks makes up a molecule’s *mass spectrum*, and is commonly represented as a plot of intensities versus m/z (Figure 1, right).

2.2 Predicting mass spectra from molecules (spectrum predictors)

Fragmentation prediction. A complex but physically grounded strategy is to model the bond breakage processes occurring in the collision cell (Figure 2A). Examples include MetFrag [48], MAGMa [36], and CFM-ID [2], which recursively fragment molecules (either bond or atom removals) to generate fragment predictions. These methods combine expert rules and local scoring methods to enumerate molecular fragmentation trees to predict spectra. CFM-ID [2] learns subsequent fragmentation transition probabilities between fragments with an expectation maximization algorithm to determine intensities at each fragment. Rule based methods and full tree enumeration reduce the flexibility of these approaches, and along with the inherent ambiguity in the fragmentation process, limit this strategy’s overall accuracy and speed.

Binned prediction. An increasingly popular and straightforward approach to spectra prediction is to map molecules to discretized 1D mass spectra from either molecular fingerprint [46] or graph inputs [51, 54] (Figure 2B). Specifically, these methods divide the m/z axis into fixed-width “bins” and predict an aggregate statistic of the peaks found in each bin (such as their max or summed intensity). While more flexible and end-to-end than fragmentation-based approaches, these methods do not impose the same physical constraints or shared information across fragments, making them less interpretable and susceptible to making invalid predictions.

Formula prediction. We introduce the strategy of predicting spectra at the level of chemical formulae, an intermediate between binned and fragmentation prediction (Figure 2C). Simultaneous to our work, two groups have separately explored formula prediction strategies [31, 55]. However, to generate plausible subformulae candidates, they either generate a fixed vocabulary of formulae [31] or restrict their model to molecules under 48 atoms for exhaustive enumeration [55], which is smaller than many compounds of interest. We overcome the combinatorial problem of formula generation using prefix trees, allowing our method to scale and eliminating the need for large, fixed vocabularies.

2.3 Mass spectrum libraries

Spectrum predictors are most useful in building large *in silico* libraries of molecule spectra to augment the small size of existing databases (on the order of 10^4). An emerging application is to determine the properties of unidentified molecules directly from their mass spectra for drug discovery applications

by leveraging such spectra libraries [42]. Another common application of spectra libraries is to infer an unknown molecule’s structure from a newly observed spectrum by *retrieval*: A database of many measured spectra (and corresponding molecules) is curated, and then newly observed spectra are matched to the existing spectra in this database using a fixed or learned spectral distance function, such as cosine distance [5, 22]. In practice, the retrieval process is constrained to choosing among *isomers* (i.e., molecules with the same chemical formula but different bond configurations) due to the high resolution of modern mass spectrometers (i.e., absolute errors on the order of 10^{-4} to 10^{-3} m/z for MS1 measurements) [13, 30, 49]. Bittremieux et al. [6] suggest that only 13% of spectra measured from clinical samples may be identifiable given current elucidation tools, up from 2% in 2014.

Given the use cases of spectra libraries, we focus upon evaluating spectrum predictors in terms of both their accuracy of prediction, using metrics such as “cosine similarity”, and also the ability of spectra libraries to directly assist with retrieval in §4.3.

3 Model

Here, we describe our model, SCARF, for predicting mass spectra from precursor molecules via first predicting subformulae of the precursor molecule, referred to as *product formulae*. Building upon the notation introduced in the previous section, we continue to denote precursor molecules¹ as $\mathcal{M} \in \mathcal{X}$, and their associated formulae vector as $\mathcal{F} \in \mathbb{N}_0^e$, defining at each position, $j \in \{1, \dots, e\}$, the count of each possible chemical element present, \mathcal{F}_j (with zero indicating none of that chemical element is present). Likewise, we define the set of n product formulae as $\{\mathbf{f}^i\}_{i=1}^n$, and associate with each an intensity, y^i . Note that the mass² corresponding to a given formula (and as such the x-axis location of the peak on a mass spectrum) is determined deterministically from the counts of each elements present.

At a high level, SCARF generates mass spectra through the composition of two learned functions:

$$\{(\mathbf{f}^i, y^i)\}_{i=1}^n = g_{\theta}^{\text{Weave}} \left(g_{\theta}^{\text{Thread}}(\mathcal{M}), \mathcal{M} \right), \quad (1)$$

first mapping from the original molecule to a set of product formulae, $g_{\theta}^{\text{Thread}} : \mathcal{M} \mapsto \{\mathbf{f}^i\}_{i=1}^n$, and then mapping from this set of formulae (and the original molecule) to the respective intensities, $g_{\theta}^{\text{Weave}} : (\{\mathbf{f}^i\}_{i=1}^n, \mathcal{M}) \mapsto \{(\mathbf{f}^i, y^i)\}_{i=1}^n$. The particularities of both functions are described in detail below. Specific architectures and hyperparameters used are deferred to the appendix; model code can be found at <https://github.com/samgoldman97/ms-pred>.

3.1 SCARF-Thread : Generating product formulae via generating prefix trees

SCARF-Thread is tasked to learn a mapping to the set of product formulae, $\{\mathbf{f}^i\}_{i=1}^n$, given the original molecule. Naively, one might try to define this model autoregressively, predicting the set formula by formula, chemical element by chemical element. For example, if the product formulae set was $\{\text{C}_7\text{OH}_4, \text{C}_7\text{OH}_6, \text{C}_7\text{O}_2\text{H}_8\}$, one would start by predicting the number of carbon atoms of the first formula (i.e., 7), then conditioned on this the number of oxygens (i.e., 1), and then the number of hydrogens (i.e., 4), before doing the same thing for the next product formula (C_7OH_6), and so on and so forth until all the atom counts of all the product formulae were specified. However, such an approach soon runs into a number of problems as (i) the predictions are not invariant to set and ordering permutations; (ii) the time complexity of prediction would scale poorly, being proportional to both the number of elements and number of product formulae (i.e., $\mathcal{O}(e \times n)$); and (iii) the predictions would likely contain duplicates.

We therefore take a different approach. We observe that many of the product formulae have identical counts for common elements, and, as such, the set of all product formulae for an individual molecule

¹We model and discuss uncharged molecules and formulae, despite mass spectrometry measuring the masses of adduct *ions*. In practice, we reduce all molecules to uncharged candidates by simply shifting all the spectra weights by the m/z of their respective adducts, which we assume to be equal to the (known) adduct of the parent molecule.

²We assume singly charged adducts (as is common practice, [2]), such that masses and mass-to-charge ratios are interchangeable.

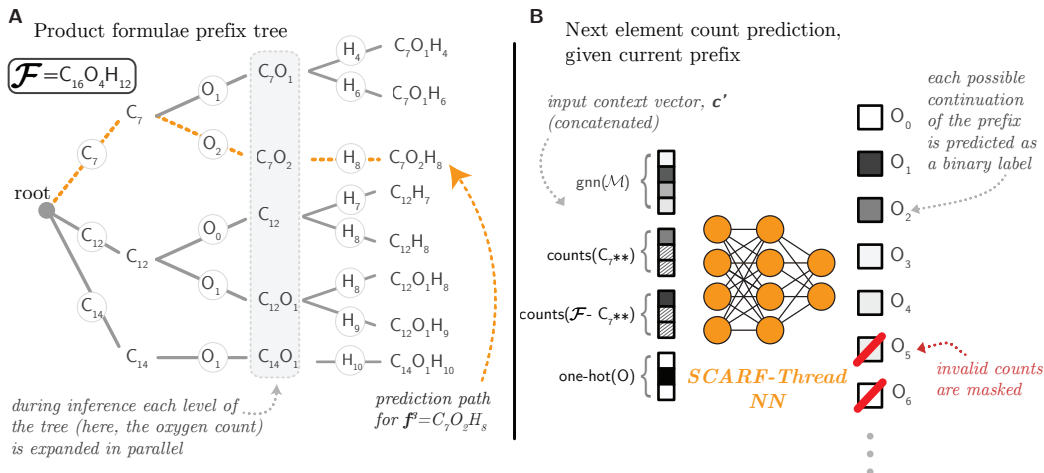


Figure 3: Illustration of the SCARF-Thread architecture. **A.** The formulae of the product fragments can be represented using a prefix tree. SCARF-Thread predicts this tree for new molecules at test time. It does so by expanding each node at a given depth in parallel, treating the counts of subsequent atoms as dependent only on the counts of atoms predicted so far (i.e., the prefix). **B.** The SCARF-Thread predictive task at the C_7 node from the prefix tree diagram shown in A. Here the network takes as input (i) an embedding of the overall molecule; (ii) a vector representing the counts of the atoms in the prefix so far (counts yet to be predicted are represented using a special token), (iii) the difference of the counts predicted so far from the precursor molecule, and (iv) a one-hot representation of the atom for which the counts are currently being predicted. The network predicts which counts are valid next nodes in the prefix tree (where counts that are greater than those in the original precursor molecule formula are masked out as invalid).

can be compactly represented by a prefix tree (Figure 3A). Here, edges at a given depth in this tree represent valid counts of a particular chemical element (shown in the circles). By following each path from the root node to the different leaf nodes, we can reconstruct each product formula (as the orange dashed path does for a single product formula). This means that defining a distribution over the set of product formulae is equivalent to defining a distribution over its corresponding prefix tree.

We propose SCARF-Thread as an autoregressive generator over such a prefix tree (Alg. 1). We assume that each product formula is a subset of the precursor formula, meaning that the precursor formula sets an upper bound on the maximum number of each element³. At each node in the tree (corresponding to a prefix $\mathbf{f}'_{<j}$), we pose the prediction of the set of child nodes (corresponding to the set of subsequent valid atom counts) as a multi-label binary classification problem (Figure 3B). Concretely, we use a neural network module for this task, giving it as input a context vector representing the node being expanded:

$$\mathbf{c}' = [\text{gnn}(\mathcal{M}), \text{counts}(\mathbf{f}'_{<j}), \text{counts}(\mathcal{F} - \mathbf{f}'_{<j}), \text{one-hot}(j)], \quad (2)$$

where $\text{gnn}(\cdot)$ specifies a neural encoding of the molecular graph (§A.4.2), $\text{counts}(\cdot)$ specifies a count-based encoding of the associated prefix (§A.4.3), and $\text{one-hot}(\cdot)$ specifies a one-hot encoding of the node’s depth (or equivalently, which element the predicted count is for).

Formulae as differences. Following Wei et al. [46], we find it helpful to not only parameterize product formulae in terms of their atom counts, but also in terms of the atoms that they have lost, i.e., their *difference* from the precursor formula. On the input side, this is already covered by including in the context vector a count-based embedding of the prefix formula minus the product formula ($\text{counts}(\mathcal{F} - \mathbf{f}'_{<j})$). However, on the output side this is achieved by combining the probabilities of a

³While it is possible for fragments to fuse together, potentially taking the count of a chemical element over the number in the original precursor formula, we postpone the extension to modeling such rare events to future work.

“forward” and a “difference” network:

$$p(f'_j = a | f'_{<j}, \mathcal{M}) = [\alpha \sigma(\text{MLP}^F(c')) + (1 - \alpha) \sigma(\text{MLP}^D(c'))]_a, \quad (3)$$

where $\text{MLP}^F(\cdot)$ and $\text{MLP}^D(\cdot)$ specify multi-layer perceptrons (MLPs) for predicting the probability of observing a count of a and $\mathcal{F}_j - a$ atoms respectively; α is a variable (output from a third, unshown network) deciding how to weight these predictions; and $\sigma(\cdot)$ is the element-wise sigmoid function.

3.2 SCARF-Weave: Predicting intensities given product formulae

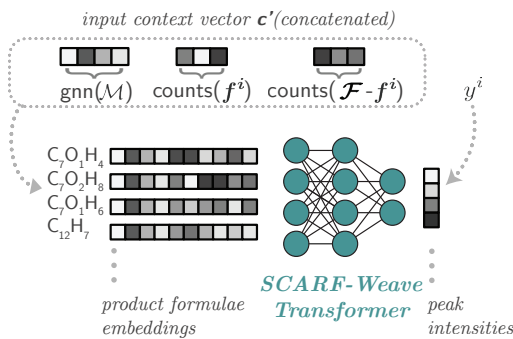


Figure 4: The SCARF-Weave network, which takes in the product formulae (e.g., predicted by SCARF-Thread) and predicts their intensities. We use a Set Transformer architecture [26], such that our model takes in the details of the other product formulae present when predicting intensities.

Given the product formulae given by SCARF-Thread described above, SCARF-Weave is used to predict their corresponding intensities. This is a set-to-set problem, and so we can use any equivariant architecture developed for this task [52, §3.1]. In our experiments, we use a Set Transformer [26, 40], which enables the model to take into account all of the formulae present in the mass spectrum (and their possible interactions) when predicting final intensities.

The main question for SCARF-Weave is therefore how best to represent the inputs to our model. We choose to do this in a similar way to the context vectors given to SCARF-Thread. Specifically, for each input we concatenate a vector embedding of the initial molecular graph with count-based embeddings of the product formula and its difference from the precursor formula (Figure 4). We again defer the particularities of the embedding functions to the Appendix (§A.4).

3.3 Training and inference

Provided with a dataset of molecules and formula-labeled mass spectra, we could train the two components of SCARF separately. However, in practice we find it beneficial to train to first train SCARF-Thread and then train SCARF-Weave on its outputs so that the distribution the latter model sees does not change between train and prediction time. SCARF-Weave is trained using a cosine loss (§A.4.5), as this most closely resembles the “retrieval” setting (§ 4.3).

SCARF-Thread is trained using the binary cross entropy losses associated with the multi-label classification tasks at each non-leaf node in the prefix tree. We use teacher forcing, i.e., we train on each level of the tree in parallel by conditioning on the ground-truth set of prefixes at each stage. When generating the set of product formulae from this model we always pick the top-300. Empirically, we find that this provides better performance than picking a variable number based on a likelihood threshold, and we hypothesize that this is because of the somewhat unbalanced nature of SCARF-Thread’s training task; prefix trees are sparse and thus only a small subset of potential atom count numbers are predicted at each step.

4 Experiments

We evaluate SCARF on the prediction of spectra (§ 4.2) as well as how these predictions can enable better identification of unknown molecules in a retrieval task (§ 4.3).

4.1 Dataset

We train and validate SCARF on two libraries: a gold standard commercial tandem mass spectrometry dataset, NIST20 [32], as well as a more heterogeneous public dataset, CANOPUS, extracted from the

Table 1: Model coverage (higher better) of true peak formulae as determined by MAGMa at various max formula cutoffs for the NIST20 and CANOPUS datasets. Best result for each column is in bold.

Dataset	NIST20				CANOPUS			
	Coverage @ 10	30	300	1000	10	30	300	1000
Random	0.008	0.024	0.232	0.533	0.003	0.015	0.130	0.337
Frequency	0.164	0.268	0.659	0.831	0.092	0.152	0.476	0.695
CFM-ID	0.198	0.281	–	–	0.169	0.267	–	–
SCARF-Thread-D	0.252	0.431	0.843	0.942	0.165	0.289	0.691	0.866
SCARF-Thread-F	0.263	0.491	0.859	0.943	0.163	0.319	0.721	0.868
SCARF-Thread	0.316	0.559	0.911	0.970	0.181	0.333	0.745	0.891

GNPS database [44] by Dührkop et al. [14] and subsequently processed by Goldman et al. [18]. We prepare both datasets by extracting and preprocessing spectra, as well as filtering to compounds that are under 1,500 Da, only contain a predefined element set, and are charged with common positive-mode adduct types (§A.2).

Overall, NIST20 contains 35,129 total spectra with 24,403 unique structures, and 12,975 unique chemical formula; CANOPUS contains 10,709 spectra, 8,553 unique structures and 5,433 unique chemical formula. Both datasets are evaluated using a structure-disjoint 80%/10%/10% train/validation/test split such that all compounds in the test set are not seen in the train and validation sets.

Annotating spectra. Herein, to standardize product formulae annotations for supervision, we utilize the knowledge of the molecule structure in combination with the MAGMa algorithm [36]. In brief, for a given molecule-spectrum pair in the training dataset, atoms are progressively removed up to a tree depth of 3 from the molecule to create sub-fragments. This creates a bank of possible chemical formulae, and each peak in the spectrum is assigned to its nearest possible formula within a mass difference of 15 parts-per-million. We emphasize that SCARF can be trained with any product formula annotations, which can be labeled [32] or inferred with varied computational strategies [13].

4.2 Spectra prediction

Predicting product formulae (SCARF-Thread). SCARF-Thread is trained and used to reconstruct prefix trees and evaluated by its ability to recover the ground truth product formula set. The set of generated product formulae is rank-ordered by the probability of each product formula and filtered to the top k predicted product formulae. The fraction of ground truth formulae (20.75 peaks on average) contained in the top- k set is computed as *coverage*.

We compare coverage achieved by SCARF-Thread to several baselines: (i) CFM-ID [2], a fragmentation based approach (§ A.3.1); (ii) a random baseline that samples product formulae from a uniform distribution; (iii) a frequency baseline, which ranks product formulae by the frequency the product formula candidate (or product formula difference) appears in the training set; and two model ablations: (iv) SCARF-Thread-D and (v) SCARF-Thread-F, which only make uni-directional atom difference or forward predictions of atom counts respectively (i.e., α in Equation 3 is fixed to 0 for (iv) and 1 for (v)).

SCARF-Thread starkly outperforms all baselines tested (Table 1). Curiously, while CFM-ID has reasonable top 10 coverage, performance does not increase at the same rate as other methods. The frequency baseline is also surprisingly strong, performing nearly as well as CFM-ID. By generating 300 peaks, SCARF-Thread is able to cover on average over 90% and 74% of true formulae in the ground truth test set for NIST20 and CANOPUS respectively. Further, weighting predictions for both the count of each atom and the difference of the complement number of atoms proves helpful as demonstrated by ablations that use either difference- or forward-only directional predictions.

Predicting mass spectra. Building off strong empirical performance in the product formulae generation task, we next evaluate the strength of SCARF-Weave for intensity prediction on the same test dataset. We compare against three baselines: a fragmentation-based approach, CFM-ID [2], and two binned prediction NEIMS models (46; §A.3.2), using either feed forward network

Table 2: Spectra prediction in terms of cosine similarity, coverage (proportion of ground-truth peaks that covered by the predictions), validity (the fraction of predicted peaks for which a chemically plausible explanation is possible), and time. Best value in each column is typeset in bold (higher is better for all metrics but time).

Dataset	NIST20			CANOPUS			Time (s)
	Cosine sim.	Coverage	Valid	Cosine sim.	Coverage	Valid	
CFM-ID	0.371	0.273	1.000	0.368	0.232	1.000	1114.7
NEIMS (FFN)	0.614	0.739	0.951	0.494	0.528	0.948	3.4
NEIMS (GNN)	0.689	0.777	0.949	0.520	0.552	0.942	4.3
SCARF	0.713	0.797	1.000	0.534	0.553	1.000	21.5

modules (FFNs), as in the original work, or graph neural network modules (GNNs) to mirror our implementation for SCARF-Weave and as described by Zhu et al. [54].

To enable fair comparison across models, we predict test spectra at 15k bins (0.1 bin resolution between 0 and 1500) with a maximum of 100 peaks for each predicted molecule and we evaluate the quality of our predictions based upon four core criteria reflecting our original desiderata of accuracy, physical-sensibleness, and speed:

1. *Cosine sim.*: Cosine similarity between the ground truth and predicted spectra, indicating spectrum prediction accuracy.
2. *Coverage*: The fraction of ground truth spectrum peaks covered by the predicted spectrum.
3. *Valid*: The fraction of predicted peaks that can be explained by a subformula of the predicted molecule.
4. *Time (s)*: The wall time it takes (using a single CPU and no batched calculations) to load the model and predict spectra for 100 randomly selected molecules.

SCARF is more accurate than all other approaches, improving cosine similarity over a GNN binned prediction approach by over 0.02 points in NIST20 and 0.01 in CANOPUS (Table 2). Further, our method is more physically-grounded insofar as all predicted peaks are guaranteed to be valid subformula, unlike the unconstrained binned approaches where nearly 5% of peak predictions cannot be explained by a valid chemical formula. Importantly, SCARF still operates 2 orders of magnitude faster than CFM-ID (Table 2). We note that the heterogeneity and reduced dataset size of CANOPUS leads to substantially worse absolute performance on this dataset across all models.

4.3 Retrieval

A key application for forward spectrum prediction is to use predicted spectra to determine the most plausible molecular structure assignment. We posit forward spectrum prediction models should be particularly helpful in differentiating structurally similar molecules and design a retrieval task to showcase such potential. For each test set molecule, we extract 49 potential "decoy" options based upon the most structurally similar *isomers* (i.e., compounds with the same precursor formula) within PubChem [24] as judged by Tanimoto similarity using Morgan fingerprints. We predict the spectra for all molecules and rank them according to their similarity to the ground truth spectrum, computing the *accuracy* for retrieval. Herein, we specifically emphasize models and retrieval on the NIST20 dataset, it is a much larger and higher quality dataset.

SCARF reaches a top-1 and top-5 retrieval accuracy in this task of 18.4% and 54.6% respectively, representing an improvement over the second best method NEIMS (GNN), which achieved top-1 and top-5 accuracies of 16.9% and 51.5% (Figure 5A). This relative ranking is consistent with performance on cosine similarity. We highlight two specific example predictions for which SCARF correctly identifies the true molecule in contrast to the baseline methods (Figure 5B-C), with randomly sampled test set predictions selected in the Appendix (Figure 6). We repeat similar experiments within CANOPUS, but find that cosine similarity performance is uncorrelated with relative ranking performance; feed forward fingerprint based approaches are better at retrieval, despite relatively weak

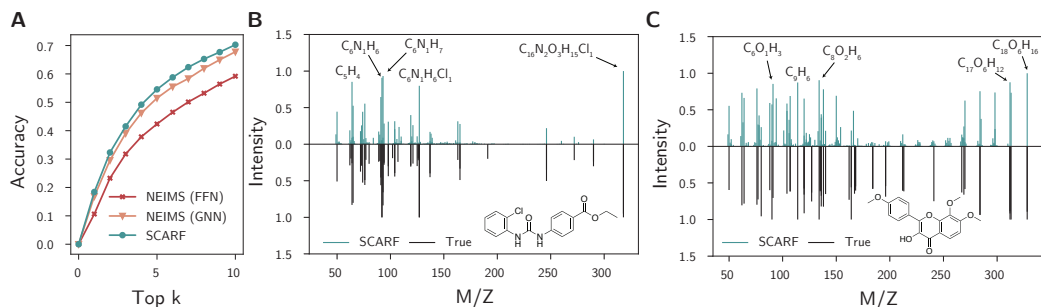


Figure 5: SCARF enables more accurate retrieval of ground truth molecules within the NIST20 dataset. **A.** Average retrieval accuracy of SCARF at various Top K thresholds. **B-C.** Example spectrum predictions made by SCARF (top) compared to the ground truth spectrum (bottom). The 5 predicted highest-intensity peaks are annotated with the chemical formula that SCARF provides to explain its prediction. The full molecule is shown inset. Further examples are in the Appendix (Figure 6).

cosine similarity (§A.1). This result underscores previous observations regarding how database and model biases can skew retrieval results under certain settings [21].

5 Related work

Forward vs backward models. Computational tools to identify mass spectra are often divided into two categories: forward and backward models. Forward models, i.e., spectrum predictors, such as SCARF or the methods discussed in Section 2, operate in the causal direction and try to predict the spectrum given the molecule. Backward models work in the opposite direction, by starting from the spectrum and predicting features or even the full structure of the molecule. Early backward models used heuristics, expert rules, and even neural networks [8, 10, 38]. Such approaches have more recently been augmented with kernel methods and more modern, deep representation learning techniques [12, 16, 18, 43]. These models are complementary to spectrum predictors and provide practitioners ways to validate forward predictions.

Mass spectra for proteomics. Although this paper has focused on small molecules, similar trends of deep representation learning for mass spectra are also emerging in the adjacent field of proteomics [50], with Shouman et al. [37] recently proposing a benchmark challenge in this domain. While small molecule and protein spectra are similar, proteomics spectra tend to be more easily predicted as fragments are often formed at peptide bonds. We believe adapting SCARF to this task would be an interesting direction for future work.

Neural set generation. Our work is also related to methods for modeling sets and multisets. SCARF-Thread generates a set as output, which has been studied elsewhere in the context of n-gram generation [41], object detection [29, 53], and point cloud generation [25]. The product formulae sets we generate, however, are different to those considered in these other task; in our setting, each member of the set (i.e., individual formulae) represents a multiset of atom types (i.e., multiple carbons, multiple hydrogens, etc.) and is constrained physically by the precursor formulae.

6 Conclusion

In this paper we introduced SCARF, an approach utilizing prefix tree data structures to efficiently decode mass spectra from molecules. By first predicting product formulae and then assigning these formulae intensities, we are able to combine the advantages of previous neural and fragment based approaches, providing fast and physically grounded predictions. We show how these resulting predictions are both more accurate in predicting experimentally-observed spectra and better able to identify and label unknown spectra in a retrieval task.

In term of limitations, our model is data dependent, as indicated by the relative performance across the NIST20 and CANOPUS datasets. SCARF is also highly reliant upon the quality of product formula label assignment. The current commercial status of mass spectrometry training data poses a barrier to entry, and identifying high quality public domain data will be important for future studies.

Future directions will involve more carefully modeling covariates (e.g., collision energies), grounding product formulae in molecular graph substructures, and utilizing such models to augment inverse spectrum-to-molecule annotation tools.

Acknowledgements

We thank members of the Coley Research Group, as well as Michael Murphy, for helpful discussions and comments. S.G. thanks the MIT-Takeda Program for financial support. J.B., J.X., and C.W.C. thank the Machine Learning for Pharmaceutical Discovery and Synthesis consortium for additional support.

References

- [1] Takuya Akiba, Shotaro Sano, Toshihiko Yanase, Takeru Ohta, and Masanori Koyama. Optuna: A next-generation hyperparameter optimization framework. In *Proceedings of the 25th ACM SIGKDD international conference on knowledge discovery & data mining*, pages 2623–2631, 2019.
- [2] Felicity Allen, Russ Greiner, and David Wishart. Competitive fragmentation modeling of ESI-MS/MS spectra for putative metabolite identification. *Metabolomics*, 11(1):98–110, 2015.
- [3] Peter W Battaglia, Jessica B Hamrick, Victor Bapst, Alvaro Sanchez-Gonzalez, Vinicius Zambaldi, Mateusz Malinowski, Andrea Tacchetti, David Raposo, Adam Santoro, Ryan Faulkner, Caglar Gulcehre, Francis Song, Andrew Ballard, Justin Gilmer, George Dahl, Ashish Vaswani, Kelsey Allen, Charles Nash, Victoria Langston, Chris Dyer, Nicolas Heess, Daan Wierstra, Pushmeet Kohli, Matt Botvinick, Oriol Vinyals, Yujia Li, and Razvan Pascanu. Relational inductive biases, deep learning, and graph networks. *arXiv preprint arXiv:1806.01261*, 2018.
- [4] Anelize Bauermeister, Helena Mannocho-Russo, Letícia V Costa-Lotufu, Alan K Jarmusch, and Pieter C Dorrestein. Mass spectrometry-based metabolomics in microbiome investigations. *Nature Reviews Microbiology*, 20(3):143–160, 2022.
- [5] Wout Bittremieux, Robin Schmid, Florian Huber, Justin J J van der Hooft, Mingxun Wang, and Pieter C Dorrestein. Comparison of cosine, modified cosine, and neutral loss based spectrum alignment for discovery of structurally related molecules. *Journal of the American Society for Mass Spectrometry*, 33(9):1733–1744, 2022.
- [6] Wout Bittremieux, Mingxun Wang, and Pieter C Dorrestein. The critical role that spectral libraries play in capturing the metabolomics community knowledge. *Metabolomics*, 18(12):94, 2022.
- [7] Michael M Bronstein, Joan Bruna, Taco Cohen, and Petar Veličković. Geometric deep learning: Grids, groups, graphs, geodesics, and gauges. *arXiv preprint arXiv:2104.13478*, 2021.
- [8] Bruce Buchanan, Georgia Sutherland, and Edward A. Feigenbaum. Heuristic Dendral: A program for generating explanatory hypotheses. *Machine Intelligence*, 4:209–254, 1969.
- [9] Jing Chen, Yi Chen, Yang Jiang, Hua Fu, Bin Xin, and Yu-Fen Zhao. Rearrangement of P-N to P-O bonds in mass spectra of N-diisopropoxyphosphoryl amino acids/alcohols. *Rapid Communications in Mass Spectrometry*, 15(20):1936–1940, 2001.
- [10] Bo Curry and David E. Rumelhart. MSnet: A neural network which classifies mass spectra. *Tetrahedron Computer Methodology*, 3(3-4):213–237, 1990.
- [11] Daniel P Demarque, Antonio EM Crotti, Ricardo Vessecchi, João LC Lopes, and Norberto P Lopes. Fragmentation reactions using electrospray ionization mass spectrometry: an important tool for the structural elucidation and characterization of synthetic and natural products. *Natural Product Reports*, 33(3):432–455, 2016.

- [12] Kai Dührkop, Huibin Shen, Marvin Meusel, Juho Rousu, and Sebastian Böcker. Searching molecular structure databases with tandem mass spectra using CSI:FingerID. *Proceedings of the National Academy of Sciences*, 112(41):12580–12585, 2015.
- [13] Kai Dührkop, Markus Fleischauer, Marcus Ludwig, Alexander A. Aksenov, Alexey V. Melnik, Marvin Meusel, Pieter C. Dorrestein, Juho Rousu, and Sebastian Böcker. SIRIUS 4: a rapid tool for turning tandem mass spectra into metabolite structure information. *Nature Methods*, 16(4), 2019.
- [14] Kai Dührkop, Louis-Félix Nothias, Markus Fleischauer, Raphael Reher, Marcus Ludwig, Martin A. Hoffmann, Daniel Petras, William H. Gerwick, Juho Rousu, and Pieter C. Dorrestein. Systematic classification of unknown metabolites using high-resolution fragmentation mass spectra. *Nature Biotechnology*, 39(4):462–471, 2021.
- [15] William Falcon and The PyTorch Lightning team. PyTorch Lightning, 3 2019. URL <https://github.com/Lightning-AI/lightning>.
- [16] Ziling Fan, Amber Alley, Kian Ghaffari, and Habtom W. Ressom. MetFID: artificial neural network-based compound fingerprint prediction for metabolite annotation. *Metabolomics*, 16(10):104, 2020. doi: 10.1007/s11306-020-01726-7.
- [17] J Gasteiger, W Hanebeck, and K P Schulz. Prediction of mass spectra from structural information. *Journal of chemical information and computer sciences*, 32(4):264–271, 1992.
- [18] Samuel Goldman, Jeremy Wohlwend, Martin Stražar, Guy Haroush, Ramnik J. Xavier, and Connor W. Coley. Annotating metabolite mass spectra with domain-inspired chemical formula transformers. *bioRxiv*, 2022. doi: 10.1101/2022.12.30.522318. URL <https://www.biorxiv.org/content/early/2022/12/31/2022.12.30.522318>.
- [19] Ian Goodfellow, Yoshua Bengio, and Aaron Courville. *Deep Learning*. The MIT Press, 2016.
- [20] William L Hamilton. Graph representation learning. *Synthesis Lectures on Artificial Intelligence and Machine Learning*, 14(3):1–159, 2020.
- [21] Martin A Hoffmann, Fleming Kretschmer, Marcus Ludwig, and Sebastian Böcker. Mad Hatter correctly annotates 98% of small molecule tandem mass spectra searching in PubChem. *Metabolites*, 13(3):314, 2023.
- [22] Florian Huber, Lars Ridder, Stefan Verhoeven, Jurriaan H Spaaks, Faruk Diblen, Simon Rogers, and Justin J J van der Hooft. Spec2Vec: Improved mass spectral similarity scoring through learning of structural relationships. *PLoS computational biology*, 17(2):e1008724, 2021.
- [23] Franziska Hufsky, Kerstin Scheubert, and Sebastian Böcker. Computational mass spectrometry for small-molecule fragmentation. *TrAC Trends in Analytical Chemistry*, 53:41–48, 2014.
- [24] Sunghwan Kim, Paul A. Thiessen, Evan E. Bolton, Jie Chen, Gang Fu, Asta Gindulyte, Lianyi Han, Jane He, Siqian He, and Benjamin A. Shoemaker. PubChem substance and compound databases. *Nucleic Acids Research*, 44(D1):D1202–D1213, 2016.
- [25] Adam R Kosiorek, Hyunjik Kim, and Danilo J Rezende. Conditional set generation with transformers. In *Workshop on Object-Oriented Learning at ICML 2020*, 2020.
- [26] Juho Lee, Yoonho Lee, Jungtaek Kim, Adam Kosiorek, Seungjin Choi, and Yee Whye Teh. Set transformer: A framework for attention-based permutation-invariant neural networks. In *Proceedings of the 36th International Conference on Machine Learning*, pages 3744–3753, 2019.
- [27] Yujia Li, Daniel Tarlow, Marc Brockschmidt, and Richard Zemel. Gated graph sequence neural networks. In *International Conference on Learning Representations*, 2016.
- [28] Richard Liaw, Eric Liang, Robert Nishihara, Philipp Moritz, Joseph E Gonzalez, and Ion Stoica. Tune: A research platform for distributed model selection and training. *ICML 2018 AutoML Workshop*, 2018.

- [29] Francesco Locatello, Dirk Weissenborn, Thomas Unterthiner, Aravindh Mahendran, Georg Heigold, Jakob Uszkoreit, Alexey Dosovitskiy, and Thomas Kipf. Object-centric learning with slot attention. In *Advances in Neural Information Processing Systems 33*, 2020.
- [30] Marcus Ludwig, Louis-Félix Nothias, Kai Dührkop, Irina Koester, Markus Fleischauer, Martin A. Hoffmann, Daniel Petras, Fernando Vargas, Mustafa Morsy, and Lihini Aluwihare. Database-independent molecular formula annotation using Gibbs sampling through ZODIAC. *Nature Machine Intelligence*, 2(10):629–641, 2020.
- [31] Michael Murphy, Stefanie Jegelka, Ernest Fraenkel, Tobias Kind, David Healey, and Thomas Butler. Efficiently predicting high resolution mass spectra with graph neural networks. *arXiv preprint arXiv:2301.11419*, 2023.
- [32] NIST. Tandem Mass Spectral Library. NIST, 2020. URL <https://www.nist.gov/programs-projects/tandem-mass-spectral-library>.
- [33] Adam Paszke, Sam Gross, Francisco Massa, Adam Lerer, James Bradbury, Gregory Chanan, Trevor Killeen, Zeming Lin, Natalia Gimelshein, Luca Antiga, Alban Desmaison, Andreas Köpf, Edward Yang, Zach DeVito, Martin Raison, Alykhan Tejani, Sasank Chilamkurthy, Benoit Steiner, Lu Fang, Junjie Bai, and Soumith Chintala. PyTorch: An imperative style, high-performance deep learning library. *arXiv preprint arXiv:1912.01703*, 2019.
- [34] Robert A Quinn, Alexey V Melnik, Alison Vrbanac, Ting Fu, Kathryn A Patras, Mitchell P Christy, Zsolt Bodai, Pedro Belda-Ferre, Anupriya Tripathi, Lawton K Chung, et al. Global chemical effects of the microbiome include new bile-acid conjugations. *Nature*, 579(7797): 123–129, 2020.
- [35] RDKit Team. RDKit: Open-source cheminformatics, 2019. URL <https://www.rdkit.org/>.
- [36] Lars Ridder, Justin JJ van der Hooft, and Stefan Verhoeven. Automatic compound annotation from mass spectrometry data using MAGMa. *Mass Spectrometry*, 3(Spec Iss 2):S0033, 2014.
- [37] Omar Shouman, Wassim Gabriel, Victor-George Giurcoiu, Vitor Sternlicht, and Mathias Wilhelm. PROSPECT: Labeled tandem mass spectrometry dataset for machine learning in proteomics. In *Thirty-sixth Conference on Neural Information Processing Systems Datasets and Benchmarks Track*, 2022.
- [38] Georgia Sutherland. Dendral-a computer program for generating and filtering chemical structures. Technical report, Stanford University, Department of Computer Science, 1967.
- [39] Matthew Tancik, Pratul P Srinivasan, Ben Mildenhall, Sara Fridovich-Keil, Nithin Raghavan, Utkarsh Singhal, Ravi Ramamoorthi, Jonathan T Barron, and Ren Ng. Fourier features let networks learn high frequency functions in low dimensional domains. In *Advances in Neural Information Processing Systems 33*, pages 7537–7547, 2020.
- [40] Ashish Vaswani, Noam Shazeer, Niki Parmar, Jakob Uszkoreit, Llion Jones, Aidan N Gomez, Lukasz Kaiser, and Illia Polosukhin. Attention is all you need. In *Advances in Neural Information Processing Systems 30*, pages 5998–6008, 2017.
- [41] Oriol Vinyals, Samy Bengio, and Manjunath Kudlur. Order matters: Sequence to sequence for sets. In *International Conference on Learning Representations*, 2016.
- [42] Gennady Voronov, Abe Frandsen, Brian Bargh, David Healey, Rose Lightheart, Tobias Kind, Pieter Dorrestein, Viswa Colluru, and Thomas Butler. MS2Prop: A machine learning model that directly predicts chemical properties from mass spectrometry data for novel compounds. *bioRxiv*, 2022. doi: 10.1101/2022.10.09.511482. URL <https://www.biorxiv.org/content/early/2022/10/10/2022.10.09.511482>.
- [43] Gennady Voronov, Rose Lightheart, Joe Davison, Christoph A. Krettler, David Healey, and Thomas Butler. Multi-scale Sinusoidal Embeddings Enable Learning on High Resolution Mass Spectrometry Data. *arXiv preprint arXiv:2207.02980*, 2022.

- [44] Mingxun Wang, Jeremy J. Carver, Vanessa V. Phelan, Laura M. Sanchez, Neha Garg, Yao Peng, Don Duy Nguyen, Jeramie Watrous, Clifford A. Kapon, and Tal Luzzatto-Knaan. Sharing and community curation of mass spectrometry data with Global Natural Products Social Molecular Networking. *Nature biotechnology*, 34(8):828–837, 2016.
- [45] Minjie Wang, Da Zheng, Zihao Ye, Quan Gan, Mufei Li, Xiang Song, Jinjing Zhou, Chao Ma, Lingfan Yu, Yu Gai, Tianjun Xiao, Tong He, George Karypis, Jinyang Li, and Zheng Zhang. Deep graph library: A graph-centric, highly-performant package for graph neural networks. *arXiv preprint arXiv:1909.01315*, 2019.
- [46] Jennifer N. Wei, David Belanger, Ryan P. Adams, and D. Sculley. Rapid prediction of electron-ionization mass spectrometry using neural networks. *ACS Central Science*, 5(4):700–708, 2019.
- [47] David S. Wishart. Metabolomics for investigating physiological and pathophysiological processes. *Physiological Reviews*, 99(4):1819–1875, 2019. doi: 10.1152/physrev.00035.2018.
- [48] Sebastian Wolf, Stephan Schmidt, Matthias Müller-Hannemann, and Steffen Neumann. In silico fragmentation for computer assisted identification of metabolite mass spectra. *BMC Bioinformatics*, 11(1):148, 2010. doi: 10.1186/1471-2105-11-148.
- [49] Shipei Xing, Sam Shen, Banghua Xu, and Tao Huan. Molecular formula discovery via bottom-up MS/MS interrogation. *bioRxiv*, 2022. doi: 10.1101/2022.08.03.502704. URL <https://www.biorxiv.org/content/early/2022/08/05/2022.08.03.502704>.
- [50] Melih Yilmaz, William Fondrie, Wout Bittremieux, Sewoong Oh, and William S. Noble. De novo mass spectrometry peptide sequencing with a transformer model. In *Proceedings of the 39th International Conference on Machine Learning*, pages 25514–25522, 2022.
- [51] Adamo Young, Bo Wang, and Hannes Röst. MassFormer: Tandem Mass Spectrum Prediction with Graph Transformers. *arXiv preprint arXiv:2111.04824*, 2021.
- [52] Manzil Zaheer, Satwik Kottur, Siamak Ravanbakhsh, Barnabas Poczos, Ruslan Salakhutdinov, and Alexander Smola. Deep sets. In *Advances in Neural Information Processing Systems 30*, pages 3391–3401, 2017.
- [53] Yan Zhang, Jonathon Hare, and Adam Prugel-Bennett. Deep set prediction networks. In *Advances in Neural Information Processing Systems 32*, 2019.
- [54] Hao Zhu, Liping Liu, and Soha Hassoun. Using Graph Neural Networks for Mass Spectrometry Prediction. In *Machine Learning for Molecules Workshop at NeurIPS 2020*, 2020.
- [55] Richard Licheng Zhu and Eric Jonas. Rapid approximate subset-based spectra prediction for electron ionization-mass spectrometry. *Analytical Chemistry*, 2023.

A Appendix

A.1 Extended results

We benchmark models in terms of retrieval accuracy as described (§ 4.3) for both the NIST20 and CANOPUS (Table 3, 4).

Table 3: NIST20 spectra prediction retrieval top-k accuracy for different values of k.

Top-k	1	2	3	4	5	6	7	8	9	10
NEIMS (FFN)	0.106	0.233	0.318	0.378	0.424	0.465	0.501	0.532	0.564	0.592
NEIMS (GNN)	0.169	0.296	0.391	0.462	0.515	0.555	0.584	0.620	0.650	0.678
SCARF	0.184	0.323	0.415	0.492	0.546	0.588	0.624	0.653	0.677	0.703

Table 4: CANOPUS spectra prediction retrieval top-k accuracy for different values of k.

Top-k	1	2	3	4	5	6	7	8	9	10
NEIMS (FFN)	0.212	0.330	0.412	0.469	0.510	0.543	0.569	0.590	0.613	0.636
NEIMS (GNN)	0.187	0.302	0.370	0.427	0.470	0.514	0.550	0.586	0.613	0.635
SCARF	0.112	0.233	0.320	0.369	0.425	0.470	0.515	0.552	0.582	0.613

We showcase additional spectra predictions from our model trained on NIST20 in Figure 6.

A.2 Dataset preparation

NIST20 [32] is prepared by extracting all positive-mode experimental spectra collected in higher-energy collision-induced dissociation (HCD) mode (i.e., collected on Orbitrap mass spectrometers). Spectra are filtered, keeping those for which the associated molecule (M) has (i) a mass under 1,500 Da, (ii) contains only atoms from a predefined element set (i.e., "C", "N", "P", "O", "S", "Si", "I", "H", "Cl", "F", "Br", "B", "Se", "Fe", "Co", "As", "Na", "K"), and (iii) is charged with common adduct types (i.e., "[M+H]+", "[M+Na]+", "[M+K]+", "[M-H2O]+", "[M+NH3+H]+", and "[M-2H2O+H]+"). Because non-standard empirical spectra databases [44] often do not include the measured collision energies, we pool all collision energies for each compound-adduct pairing to create a single spectrum. We refer the reader to Young et al. [51] for detailed instructions for purchasing and extracting the NIST20 dataset.

All spectrum intensities are square-root transformed to provide higher weighting to lower intensity peaks, normalized to a maximum intensity of 1 (i.e., dividing by maximum intensity), filtered to exclude any noise peaks with normalized intensity under 0.003, and subsetted to only the top 50 highest intensity peaks. All peaks are mass-shifted by the weight of the parent adduct (i.e., if the spectrum is "[M+H]+", the weight of a proton is subtracted from each child peak).

A.2.1 Product formulae assignments

Because the precursor ion and adduct species are known for the training dataset, we subtract the precursor adduct mass from every peak in the training set, and attempt to annotate each peak with a plausible product formula (i.e., a subset of the true precursor formula).

We opt to constrain the training product formulae to be subsets of contiguous heavy atoms of the parent molecule as derived with the MAGMa algorithm [36].

We note two important limitations of these heuristics. First, by using molecular substructures to annotate product formulae, our model is less prone to correctly identifying complex rearrangements. Second, it is also possible for adduct switching to occur. Namely, if the precursor ion has a sodium adduct ("[M+Na]+"), some of the product formulae may actually switch and acquire a hydrogen adduct instead. We assume no adduct switching in our formulation, instead focusing on the novelty

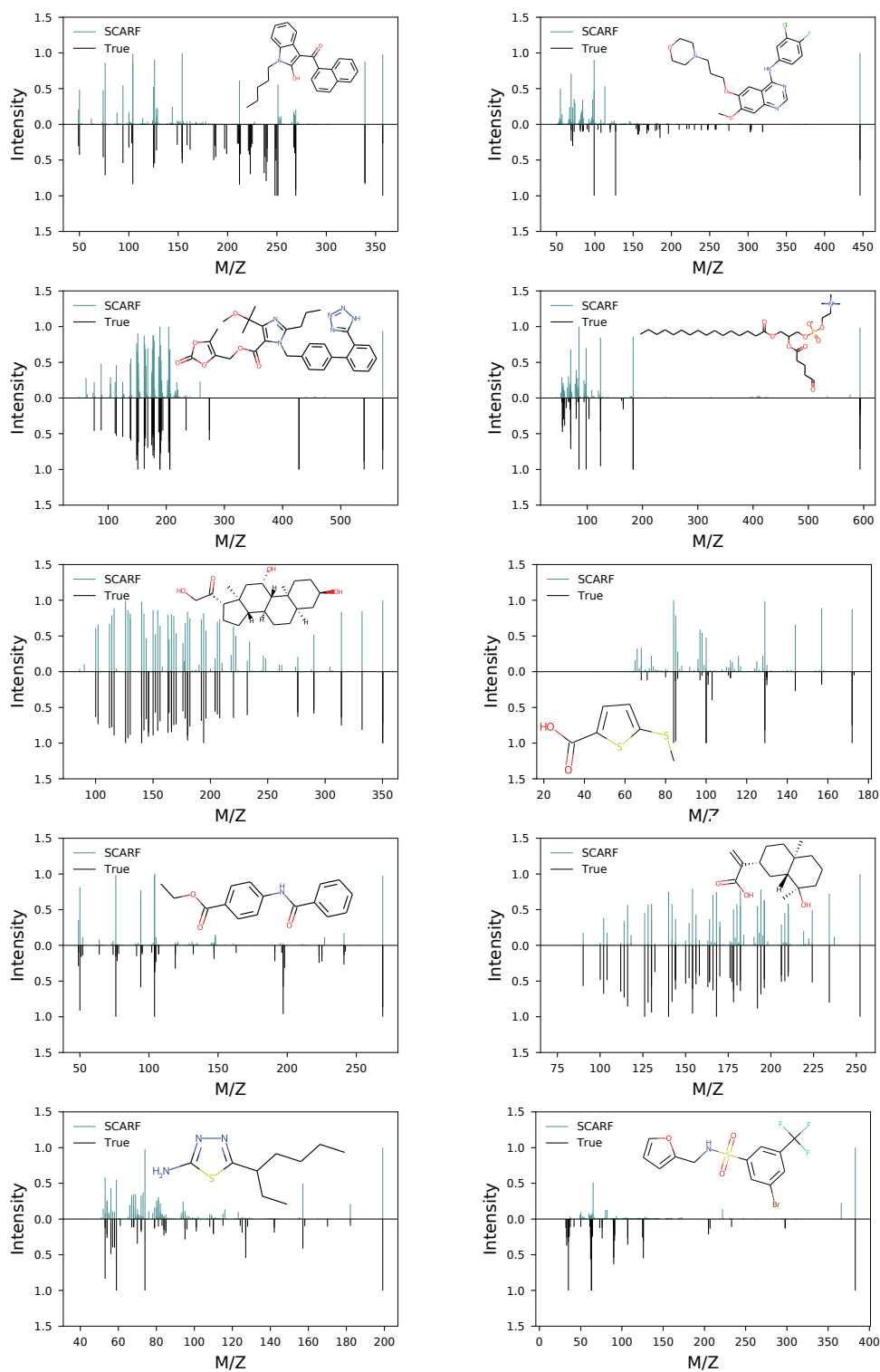


Figure 6: Example spectra predictions from the NIST20 for 10 randomly selected test molecules. The ground truth spectra are shown underneath in black, with predictions above in teal. Molecules are shown inset.

of the prefix tree decoding approach, as these represent data labeling challenges, rather than modeling challenges.

In addition, any predictive models of product formulae distributions will more closely predict spectra that would be produced on instrumentation similar to the training sets utilized [9, 11]. Given this, we encourage users of such models to treat these predictions as putative, rather than experimentally valid.

A.3 Baselines

A.3.1 CFM-ID baseline

CFM-ID [2] is a long standing and important approach to fragmentation prediction. Because CFM-ID is fit using a time intensive EM training approach on an analogous dataset, we utilize the pretrained Docker version provided by the authors in line with [31]. CFM-ID has two options for predicting molecules in either positive or negative adduct mode with "H" adducts (i.e., "[M+H]+" or "[M-H]-"). To directly compare to our method, we predict spectra in positive mode and remove hydrogens from all predicted peaks, as all training peaks are shifted by removing their adducts.

CFM-ID also produces predictions at three collision energies (i.e., low, medium, or high fragmentation). Because we opt not to include these, we merge these predictions and re-normalize the result to a maximum of 1.

A.3.2 NEIMS baseline

NEIMS [46] is a highly efficient binned spectrum prediction approach, originally developed for gas chromatography-mass spectra (GC-MS). To enable a fair comparison, we optimize its hyperparameters on our dataset and add higher resolution bins. Furthermore, we also train a graph neural network-based version "NEIMS (GNN)" (in addition to the network that more closely matches Wei et al. [46]'s original model and operates on the molecular fingerprint, "NEIMS (FFN)"). The adduct type is either concatenated to all atom features (for NEIMS (GNN)) or to the fingerprint vector (for NEIMS (FFN)).

A.4 Model details

Here, we describe details of our model's training setup, architecture, and hyperparameters that were omitted from the main text. Definitive details can also be found in the code at <https://github.com/samgoldman97/ms-pred>.

A.4.1 Training

We train each of our models on a single RTX A5000 NVIDIA GPU (CUDA Version 11.6), making use of the Torch Lightning [15] library to manage the training. SCARF-Thread and SCARF-Weave take on the order of 1.5 and 2.5 hours of wall time to train respectively.

A.4.2 Molecule encoding

Within both SCARF-Thread and SCARF-Weave, a key component is an encoding of the molecular graph using a message passing graph neural network, $\text{gnn}(\mathcal{M})$. Such graph neural network models are now well described [3, 7, 20], so we will skip a detailed explanation of them here. In our experiments, we use gated graph sequence neural networks [27]. We made use of the implementation of this network in the DGL library [45] and use as atom features those shown in Table 5 (which are computed using RDKit [35] or DGL [45]).

A.4.3 Chemical formulae representations

When forming representations of formulae (including formulae prefixes) we use a count-based encoder, $\text{counts}(\mathbf{f})$. This encoder takes in as input the counts of all individual elements in the formula (which also can be "undefined" for counts of atoms not yet specified – indicated as '*' in Figure 3B) and returns a vector representation in \mathbb{R}^d . The encoder is based upon the Fourier feature mapping proposed by Tancik et al. [39], but using only sin basis functions (to reduce the number of parameters

Table 5: Graph neural network (GNN) atom features.

Name	Description
Element type	one-hot encoding of the element type
Degree	one-hot encoding of number of bonds atom is associated with
Hybridization type	one-hot encoding of the hybridization (SP, SP2, SP3, SP3D, SP3D2)
Charge	one-hot encoding of atom’s formal charge (from -2 to 3)
Ring-system	binary flag indicating whether atom is part of a ring
Atom mass	atom’s mass as a float
Chiral tag	atom’s chiral tag as one-hot encoding
Adduct type	one-hot encoding of the adduct ion
Random walk embed steps	positional encodings of the nodes computed using DGL

required by our networks). Tancik et al. [39] has shown that such features perform better than encoding integers directly; furthermore, compared to learned representations, using Fourier features also enables us (at least in principle) to deal with counts at test time that have not been seen during training.

To be precise, each possible count, $v \in \mathbb{N}_0$, is encoded by our counts-based encoder into the vector:

$$\text{relu} \left(\left[\sin \left(\frac{2\pi v}{T_1} \right), \sin \left(\frac{2\pi v}{T_2} \right), \sin \left(\frac{2\pi v}{T_3} \right), \dots \right] \right),$$

where the periods (T_1, T_2 , etc.) are set at increasing powers of two that enable us to discriminate all possible element counts given in the input, and $\text{relu}(\cdot)$ is the rectified linear unit activation function [19, §6.3.1] such that we get positive embeddings. For the “undefined” count we learn a separate encoding of the same dimensionality.

A.4.4 Further details of SCARF-Thread

Pseudo-code for the SCARF-Thread model is shown in Algorithm 1. Note that the second for loop (on the line marked ‡) does not depend on previous iterations of the loop, so that in practice we perform this computation in parallel. At training time we use teacher forcing (§3.3), meaning the first for loop (marked †) is only run sequentially at inference time.

The function `scarf-thread-net(\cdot)` represents the network shown in Figure 3B and generates the set of subsequent valid element counts given a prefix (i.e., the child nodes of a given prefix node). As discussed in the main text, we treat this as a multi-label binary classification task and predict the binary label for each possible count using forward and difference MLPs (Eq. 3). We fix a maximum possible element count (i.e., the number of possible classes in this classification problem), $N = 160$. We do not allow product formulae to have more of a given element than is present in the precursor formula, \mathcal{F} , and we achieve this by setting the probability of these classes to zero.

Algorithm 1: Pseudo-code for SCARF-Thread, which generates prefix trees from a root node autoregressively, one level at a time.

Data: Input molecule, \mathcal{M} , with corresponding input formula, \mathcal{F} .

Result: Set of product formulae, $\rho_e = \{f^i\}_{i=1}^n$.

```

1  $h_{\mathcal{M}} \leftarrow \text{gnn}(\mathcal{M})$ ; ▷ Form embedding of precursor molecule.
2  $\rho_0 \leftarrow \{*\}$ ; ▷ Store the set of initial prefixes which is just the undefined formula, *.
3† for  $j \in [1, \dots, e]$  do ▷ Loop over all possible elements.
4    $\rho_j \leftarrow \{\}$ ; ▷ Create the set of prefixes the next time around.
5    $h_j \leftarrow \text{one-hot}(j)$ ; ▷ Encoding of which element we are predicting the count of.
6‡   for  $f'_{<j} \in \rho_{j-1}$  do (in parallel) ▷ Loop over all current prefixes.
7      $c' = [h_{\mathcal{M}}, \text{counts}(f'_{<j}), \text{counts}(\mathcal{F} - f'_{<j}), h_j]$ ; ▷ Create context vector, Eq. 2
8      $\{f_j^{i'}\}_{i'=1}^{n'} \leftarrow \text{scarf-thread-net}(c', \mathcal{F})$ ; ▷ Predict the set of valid next atom counts under this prefix.
9      $\rho_j \leftarrow \rho_j \cup \text{create-new-prefixes}(f'_{<j}, \{f_j^{i'}\}_{i'=1}^{n'})$ ; ▷ Create new prefixes for the next element.
return  $\rho_e$ 

```

A.4.5 Further details of SCARF-Weave

As discussed in the main text, SCARF-Weave is based off Lee et al. [26]’s Set Transformer. After forming the input encoding using the molecule and count-based encoder (§A.4.2 & §A.4.3), we further refine this embedding using an MLP (multi-layer perceptron) network. The output of this is passed into a series of l_3 Transformer [40] layers (§A.4.6 defines the exact number used in the experiments) with 8 attention heads each.

We use a cosine distance loss to train the parameters of SCARF-Weave. This loss is also used for the FFN and GNN baselines (Table 2). To ensure consistency with the baselines, we first project the output of SCARF-Weave into a binned histogram representation (§A.4.6 defines the number of bins used); for each bin we take the max intensity across all applicable formulae. Given a predicted binned spectra, \hat{s} , and the ground-truth binned spectra, s , the cosine distance is defined as the negative of the cosine similarity (computed using PyTorch’s `torch.cosine_similarity` function [33]):

$$\text{cos-sim}(\hat{s}, s) = \frac{\hat{s} \cdot s}{\max(\|\hat{s}\|_2 \|s\|_2, \epsilon)}, \tag{4}$$

where $\epsilon = 1 \times 10^{-8}$ is used to ensure numerical stability.

A.4.6 Hyperparameters

To enable fair comparison across models, hyperparameters were tuned for SCARF, the FFN binned prediction baseline, and the GNN binned prediction baseline. Parameters were tuned using RayTune [28] with Optuna [1] and an ASHAScheduler. Each model was allotted 50 different hyperoptimization trials for fitting. Models were hyperparameter optimized on a smaller 10,000 spectra subset of NIST20. Parameters are detailed in Table 6.

Table 6: Model and baseline hyperparameters.

Model	Parameter	Grid	Value
NEIMS (FFN)	learning rate	$[1e-4, 1e-3]$	0.00087
	learning rate scheduler	-	StepDecay (5,000)
	learning rate decay	$[0.7, 1.0]$	0.722
	dropout	$\{0.1, 0.2, 0.3\}$	0.0
	hidden size, d	$\{64, 128, 256, 512\}$	512
	layers, l	$\{1, 2, 3\}$	2
	batch size	$\{16, 32, 64, 128\}$	128
	weight decay	$\{0, 1e-6, 1e-7\}$	0
	use differences (Eq.3)	$\{\text{True}, \text{False}\}$	True
	num bins (§A.4.5)	-	15,000
NEIMS (GNN)	learning rate	$[1e-4, 1e-3]$	0.00052
	learning rate scheduler	-	StepDecay (5,000)
	learning rate decay	$[0.7, 1.0]$	0.767
	dropout	$\{0.1, 0.2, 0.3\}$	0.0
	hidden size, d	$\{64, 128, 256, 512\}$	512
	layers, l	$[1, 6]$	4
	batch size	$\{16, 32, 64\}$	64
	weight decay	$\{0, 1e-6, 1e-7\}$	$1e-7$
	use differences (Eq.3)	$\{\text{True}, \text{False}\}$	True
	num bins (§A.4.5)	-	15,000
	conv type	-	GatedGraphConv
	random walk embed steps (Table 5)	$[0, 20]$	19
	graph pooling	$\{\text{mean}, \text{attention}\}$	attention
SCARF-Thread	learning rate	$[1e-4, 1e-3]$	0.000577
	learning rate scheduler	-	StepDecay (5,000)
	learning rate decay	$[0.7, 1.0]$	0.894
	dropout	$\{0.1, 0.2, 0.3\}$	0.3
	hidden size, d	$\{128, 256, 512\}$	512
	mlp layers, l_1	$[1, 3]$	2
	gnn layers, l_2 (§A.4.2)	$[1, 6]$	4
	batch size	$\{8, 16, 32, 64\}$	16
	weight decay	$\{0, 1e-6, 1e-7\}$	$1e-6$
	use differences (Eq.3)	$\{\text{True}, \text{False}\}$	True
	conv type	-	GatedGraphConv
	random walk embed steps (Table 5)	$[0, 20]$	20
	graph pooling	$\{\text{mean}, \text{attention}\}$	mean
SCARF-Weave	learning rate	$[1e-4, 1e-3]$	0.000308
	learning rate scheduler	-	StepDecay (5,000)
	learning rate decay	$[0.7, 1.0]$	0.962
	dropout	$\{0.1, 0.2, 0.3\}$	0.2
	hidden size, d	$\{128, 256, 512\}$	512
	mlp layers, l_1 (§A.4.5)	$[1, 3]$	3
	gnn layers, l_2 (§A.4.2)	$[1, 6]$	3
	transformer layers, l_3 (§A.4.5)	$[0, 3]$	2
	batch size	$\{4, 8, 16, 32, 64\}$	32
	weight decay	$\{0, 1e-6, 1e-7\}$	0
	num bins (§A.4.5)	-	15,000
	conv type	-	GatedGraphConv
	random walk embed steps (Table 5)	$[0, 20]$	7
graph pooling	$\{\text{mean}, \text{attention}\}$	attention	